Macromolecules

COMMUNICATION TO THE EDITOR

pubs.acs.org/Macromolecules

Fluorinated Microgel-Core Star Polymers as Fluorous Compartments for Molecular Recognition

Yuta Koda, Takaya Terashima,* Akihisa Nomura, Makoto Ouchi, and Mitsuo Sawamoto*

Department of Polymer Chemistry, Graduate School of Engineering, Kyoto University, Kyotodaigaku-katsura, Nishikyo-ku, Kyoto 615-8510, Japan

Supporting Information

Design of a confined nanospace in macromolecules plays a critical role in selective molecular recognition, catalysis, and other functions.[1−3] Microgel-core star polymers[4−12] are among globular macromolecules that provide such attractive space within the microgel core, which is compartmentalized by linear arms from the outer environment to enclose and condense functional groups. They can be facilely prepared and functionalized, for example, by metal-catalyzed living radical polymerization in one pot.[13−16] With their well-defined and specific structures, star polymers carrying polar functional groups typically perform unique molecular recognition of protic guest molecules via hydrogen bonding.[6,8]

In addition to functionalization for hydrogen bonding, fluorination of organic (macro)molecules is intriguing in developing unique functions because fluorine atoms may give macromolecules with not only high thermal stability and low surface energy[17,18] but also the so-called "fluorous" character, or the incompatibility with aqueous (hydrophilic) and common organic (lipophilic) phases.[19−25] The fluorous nature typically leads to facile separation in catalysis[19−21] and stable formation of micelles and vesicles in solution.[23−25]

In this work, the unique nature encouraged us to fluorinate the microgel cores in star polymers via our metal-catalyzed living radical polymerization and core functionalization to construct nanoscale fluorinated compartments for efficient and selective molecular recognition (Scheme 1). The fluorination also serves as a highly sensitive and unique probe for not only molecular recognition but also the characterization of the core environment (diffusion, space confinement, thermal movement, etc.), which has been unknown so far, by ^{19}F nuclear magnetic resonance (NMR) and diffusion-ordered NMR spectroscopy (DOSY).[22,26,27] To our best knowledge, this is the first example to create fluorinated microgel-core star polymers for fluorous molecular recognition.

Fluorinated microgel-core star polymers (coded **P1**−**P4**) were synthesized by two steps in one pot: (A) arm synthesis by the Ru(Ind)Cl(PPh_3)$_2$-catalyzed living radical polymerization of methyl methacrylate (MMA) with a chloride initiator (ethyl α-chlorophenylacetate: ECPA), followed by (B) arm linking (core formation) with ethylene glycol dimethacrylate (EGDMA) or 2,2,3,3,4,4,5,5,6,6,7,7-dodecafluoro-1,8-octanediol dimethacrylate (12FODMA), in the presence of 1*H*,1*H*,2*H*,2*H*-perfluorooctyl methacrylate (13FOMA), which copolymerizes with these divinyl linkers to be incorporated into the microgel core network. The feed ratio (n) of 13FOMA was varied to change the fluorine contents in the core (n = [13FOMA]/[ECPA] = 0−10), while the molar ratio (m) of the bifunctional linker to the initiator (ECPA) (or the living PMMA arm) was set constant (m = [EGDMA or 12FODMA]/[ECPA] = 10). Note that the 12FODMA/13FOMA pair gives the highest core fluorine content, while the EGDMA/13FOMA pair gives cores of less fluorine and of pendent perfluoroalkyl groups alone. To efficiently create fluorine-condensed microgel core, the arm linking reaction was performed after the evaporation of MMA residue in the prepoly(MMA) synthesis.

Scheme 1. Synthesis of Fluorinated Microgel-Core Star Polymers via Ruthenium-Catalyzed Living Radical Polymerization and the Selective Molecular Recognition in the Fluorous Compartments

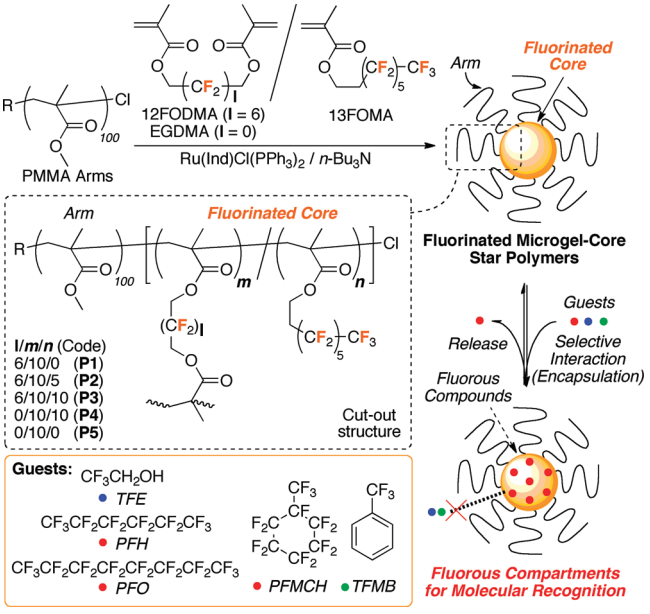

While the arm linking reaction was performed after the evaporation of MMA residue in the prepoly(MMA) synthesis.

In a typical run (Figure 1a), PMMA arms [M_n (SEC) = 13 200; M_n (NMR) = 12 900; M_w/M_n = 1.15] were smoothly linked with EGDMA and 13FOMA (m = n = 10) to give star polymers (**P4**) in high yield (∼84%). Similarly, other samples

Received: May 11, 2011
Revised: May 20, 2011
Published: June 03, 2011

(**P1**−**P3**) of varying core-fluorine contents were obtained in high yield, along with a control sample (**P5**) with a fluorine-free core from EGDMA alone (Table 1, Table S1 and Figures S1 and S2): Absolute weight-average molecular weight (M_w) = (2.92−20.0) × 10^5; arms per polymer (N_{arm}) = 13−75; and radius of gyration (R_g) = 7.0−20 nm, all based on multi-angle laser light scattering coupled with size exclusion chromatography (SEC-MALLS).

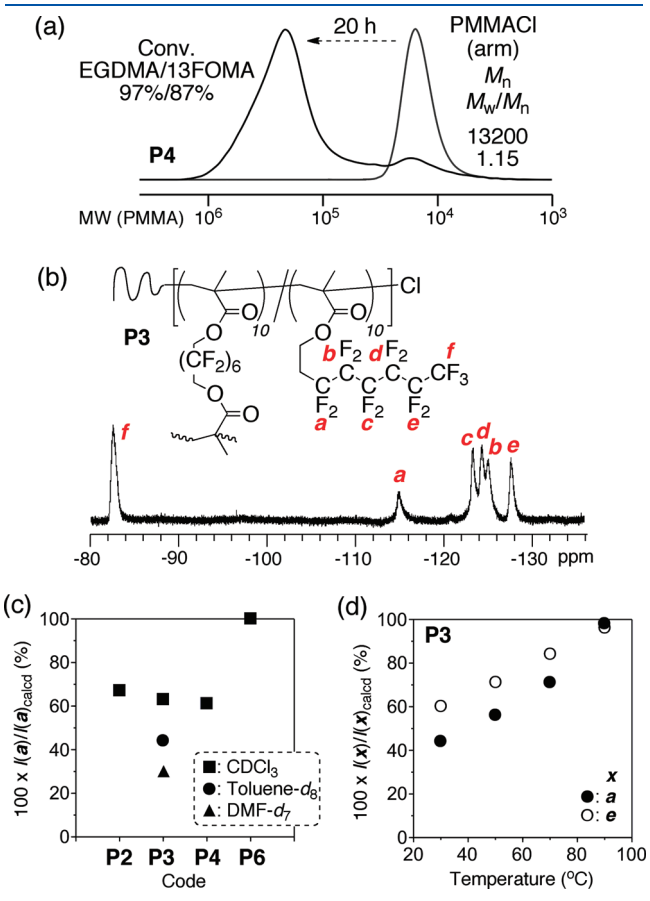

Figure 1. (a) SEC curves of **P4** prepared by Ru-catalyzed living radical polymerization of EGDMA and 13FOMA with PMMACl in toluene at 80 °C. Condition (ratio): [PMMACl]/[EGDMA]/[13FOMA]/[Ru(Ind)Cl(PPh_3)$_2$]/[*n*-Bu_3N] = 1/10/10/0.1/10. (b) ^{19}F NMR spectra (470 MHz) of **P3** in $CDCl_3$ at 30 °C. (c) Effects of solvent ($CDCl_3$, toluene-d_8, DMF-d_7) and polymers [star: **P2**; **P3**; **P4**. MMA/13FOMA (100/10) random: **P6**] on signal intensity ratio of *a* observed [$I(a)$] to *a* calculated [$I(a)_{calcd}$] in ^{19}F NMR at 30 °C. (d) Effects of temperature (30, 50, 70, 90 °C) on signal intensity ratio of *x* (= *a*, *e*) observed [$I(x)$] to *x* calculated [$I(x)_{calcd}$] in ^{19}F NMR of **P3** in toluene-d_8 (the peak assignments of *a* and *e* correspond to those in (b)).

For **P1**−**P3**, the M_w, N_{arm}, and R_g increased with increasing amount (n) of 13FOMA incorporated into the core and thus indicated an increase in core size. The number of core-bound fluorine (N_F) in **P1**−**P4** were as large as 1860−17 300, as calculated from N_{arm}, the feed ratios m and n of the core components, and their conversion: $N_F = N_{arm} \times [12m \times \text{conv}(12\text{FODMA})/100 + 13n \times \text{conv}(13\text{FOMA})/100]$. As expected, N_F increased with increasing n. Thus, by this simple methodology outlined in Scheme 1, a large number of fluorine atoms were directly and densely incorporated into a nanosize microgel core; e.g., in **P3**: N_F = 17 300; $M_w = 2.0 \times 10^6$; N_{arm} = 75 arms; N_{CF_3} = 667.

The core-bound fluorine was in turn employed as a probe to characterize the thermal movement of the core by ^{19}F NMR as a function of solvent, temperature, and the core structure (Figure 1b−d; Figures S3 and S4); for comparison, a linear random copolymers of MMA and 13FOMA was also employed, which mimics the linking units within a core (**P6**: MMA/13FOMA = 100/10; M_n(SEC) = 14 000; M_w/M_n = 1.18; N_F = 118; N_{CF_3} = 9).

All of the star polymers exhibited ^{19}F signals in $CDCl_3$ at 30 °C, but the signals from the 12FODMA units in **P1** were quite weak, indicative of the low mobility of the core components within a tight network.[7,10] For assessing the core-unit mobility, the signal intensity $I(a)$ of the innermost pendent CF_2 [−O−$(CH_2)_2$−CF_2 in 13FOMA units; peak *a*, Figure 1b] was compared with its estimated maximum [$I(a)_{calcd}$] based on the signal intensity of the pendent-end or "tip" CF_3 (peak *f*) assuming that this group can freely move even within a tight network and thus exhibit unperturbed NMR signals.

As seen in Figure 1c, $I(a)$ for **P2**−**P4** was about 60% of $I(a)_{calcd}$, whereas that for the linear control **P6** was close to $I(a)_{calcd}$. The weaker signals indicate restricted thermal movement of the core units. With **P3**, peak *a* gradually weakened and broadened with solvents in the order $CDCl_3$ < toluene-d_8 < DMF-d_7; namely, the core mobility decreased with decreasing fluorine affinity of these solvents.[20,28] $I(a)$ increased at higher temperature to reach $I(a)_{calcd}$ at 90 °C, where the core units may move as freely as in linear chains (Figure 1d; Figure S4 and Table S2). With **P3**, $I(a)/I(a)_{calcd}$ was

Table 1. Characterization of Fluorinated Microgel-Core Star Polymers[a]

code	L[a]	n[a]	conversion[b] (L/13FOMA, %)	yield$_{star}$[c] (%)	$M_{w,star}$[d] (SEC)	$M_{w,star}$[e] (MALLS)	N_{arm}[f]	R_g[e] (nm)	N_F[g]	N_{CF_3}[g]
P1	12FODMA	0	90/−	64	139 700	361 000	17	15	1860	0
P2	12FODMA	5	95/88	81	284 000	996 000	40	17	6770	173
P3	12FODMA	10	96/88	77	435 000	2 000 000	75	20	17 300	667
P4	EGDMA	10	97/87	84	306 700	1 190 000	52	12	5900	454
P5	EGDMA	0	94/−	87	123 400	292 000	13	7.0	0	0

[a] Fluorinated microgel-core star polymers (**P1**−**P5**) were prepared by ruthenium-catalyzed living radical polymerization of divinyl compounds (L: EGDMA or 12FODMA) and 13FOMA with PMMA-Cl arms (M_n ∼ 13 000, M_w/M_n = 1.15) in toluene at 80 °C: [PMMA-Cl]/[(Ind)RuCl-(PPh_3)$_2$]/[*n*-Bu_3N] = 20/200/20, m = [L]$_{add}$/[PMMA-Cl]$_0$ = 10, n = [13FOMA]$_{add}$/[PMMA-Cl]$_0$. [b] Determined by ^{1}H NMR with tetralin as an internal standard [linking time: 20 h (**P1**−**P4**); 31 h (**P5**)]. [c] Calculated from the area ratio of star polymers and arm polymers in SEC curves. [d] Weight-average molecular weight (M_w) of star polymers determined by SEC in THF with PMMA standards. [e] Absolute weight-average molecular weight [$M_{w,star}$ (MALLS)] and radius of gyration (R_g) of star polymers determined by SEC-MALLS in DMF (10 mM LiBr). [f] Arm numbers per a star polymer: N_{arm} = (weight fraction of arm polymers) × $M_{w,star}$ (MALLS)/$M_{w,arm}$ (SEC). [g] Fluorine atom numbers (N_F) and CF_3 group numbers (N_{CF_3}) per a star polymer: $N_F = N_{arm} \times [12 \times m \times \text{conv}(12\text{FODMA})/100 + 13 \times n \times \text{conv}(13\text{FOMA})/100]$; $N_{CF_3} = N_{arm} \times n \times \text{conv}(13\text{FOMA})/100$.

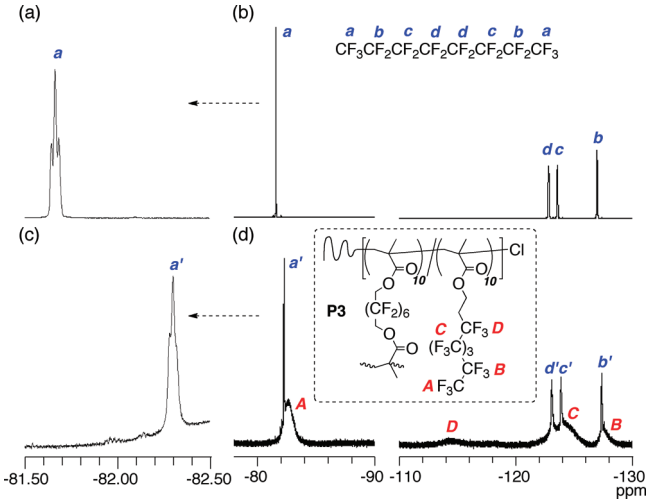

Figure 2. ^{19}F NMR (470 MHz) spectra of (a, b) PFO in $CDCl_3$ and (c, d) PFO with **P3** in DMF-d_7 at 30 °C. (a) and (c): magnified spectra of (b) and (d), respectively. The peaks of $a'-d'$ in (c) and (d) correspond to PFO encapsulated into **P3**.

smaller than $I(e)/I(e)_{calcd}$, namely, the closer the pendent CF_2 to the backbone, the more restricted its thermal movement.

The decreased mobility of the in-core pendent groups was further demonstrated by the spin−lattice relaxation time (T_1)[27] of the tip fluorine atoms (CF_3:*f*). T_1 was much smaller with **P3** (0.499 s) than with the linear counterpart **P6** (1.48 s) in $CDCl_3$ at 30 °C.

The fluorous character of the microgel core was then evaluated in molecular recognition of (per)fluorinated guest compounds, such as perfluorooctane (PFO), perfluorohexane (PFH), perfluoromethylcyclohexane (PFMCH), trifluoromethylbenzene (TFMB), and 2,2,2-trifluoroethanol (TFE) (Scheme 1). PFO, PFH, and PFMCH are "fluorous", or immiscible with DMF and DMSO, while partially miscible with $CHCl_3$.[20] Partially fluorinated, TFMB and TFE are not fluorous but regarded as hydrophobic and hydrophilic, respectively. PFO led to an emulsion when stirred in DMF-d_7 containing **P3** at room temperature for 24 h. Stirring was then stopped, and after phase separation, the transparent DMF-d_7 layer was analyzed by ^{19}F NMR (Figure 2). The solution showed fluorine signals of PFO as well as **P3**, demonstrating that its fluorous core efficiently solubilizes PFO into DMF-d_7. The CF_3 signal (a': −82.3 ppm) of PFO turned much broader than in $CDCl_3$ without **P3** (a: −81.7 ppm), indicating a strong interaction between PFO and the fluorinated core. **P3** also solubilized PFO into $CDCl_3$, while the interaction was smaller than in DMF-d_7 (Figure S5).

The "fluorous" molecular recognition by **P3** was further examined by ^{19}F DOSY in $CDCl_3$ and DMF-d_7 (Figure 3; Figure S8 and Table S4).[22,29] In the presence of **P3**, PFO showed two series of signals with diffusion coefficient (D_{NMR}) in $CDCl_3$: D_{NMR} = 1.6 × 10^{-9} and 5.2 × 10^{-10} m^2/s (Figure 3a), in contrast to a single value in a **P3**-free PFO (D_{NMR} = 2.2 × 10^{-9} m^2/s; Figure S8a). The larger value is similar to that for the star-free PFO and thus corresponds to the PFO molecules without interaction with **P3**. The smaller value was close to D_{NMR} for the **P3** core with PFO (signal *A*) but larger than that of **P3** alone (6.7 × 10^{-11} m^2/s), and thereby it is assigned to PFO interacting with **P3** (see peak a'). In DMF-d_7, only a single value of D_{NMR} was obtained for PFO even in the presence of **P3**, which was

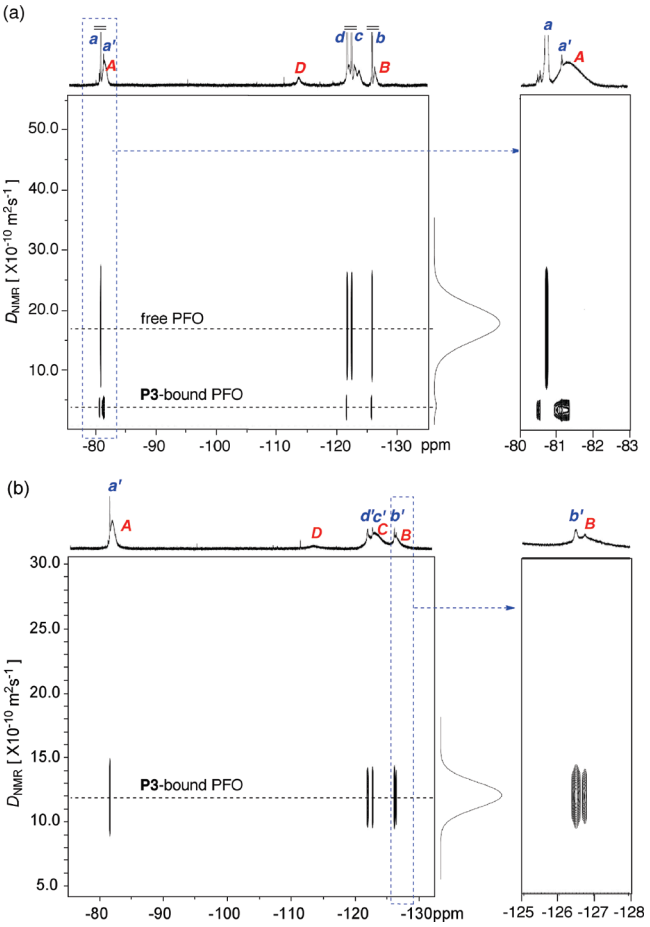

Figure 3. ^{19}F DOSY spectra (470 MHz) of PFO with **P3** in $CDCl_3$ (a) and DMF-d_7 (b) at 30 °C. The peak assignments of $a-d$, $a'-d'$, and $A-D$ correspond to those in Figure 2.

nearly identical to that for the star (Figure 3b). Thus, PFO is completely incorporated in the fluorous core in DMF-d_7, while partially in $CDCl_3$. This further suggests that the fluorous core compartment may further welcome PFO guests inside in DMF due to the originally low affinity of PFO to DMF.

In the fluorous recognition by **P3** in DMF-d_7, as many as 209 PFO molecules were entrapped in the single core (Table S3; by ^{19}F NMR). PFH and PFMCH were also good guests under the same conditions: 189 and 306 molecules per core (Figures S6 and S7; Figure 4d). However, the hydrodynamic radius (R_h) of **P3**, determined by dynamic light scattering (DLS), remained virtually unchanged upon guest incorporation or independent of the presence and the absence of PFO in DMF (33.4 vs 33.8 nm; Figure S9). These results supported that, in DMF, the fluorinated star polymer behaved a nanofluorous isolated compartment within a single star polymer molecule.

The effects of host polymer structures on the fluorous molecular recognition was further examined with **P1**−**P6** (host) and PFMCH (guest) in DMF-d_7 (Figure 4 and Figure S7). All the hosts solubilized PFMCH, while the signal shape of the tip CF_3 and the amount of the solubilized guest were strongly dependent on the host structure and the composition of cores. For all the hosts, the CF_3 signal (a) was multiplet but gradually broadened with increasing amounts of 13FOMA in the core (**P1**−**P3**), meaning that the more fluorous (or the higher in fluorine content) the core is, the stronger the host−guest

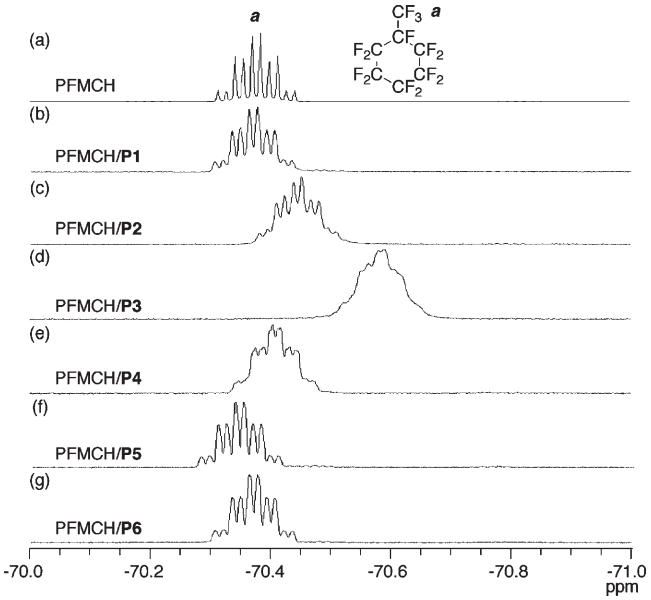

Figure 4. ^{19}F NMR (470 MHz) spectra of (a) PFMCH in $CDCl_3$ and (b−g) PFMCH with **P1**, **P2**, **P3**, **P4**, **P5**, and **P6**, respectively, in DMF-d_7 at 30 °C.

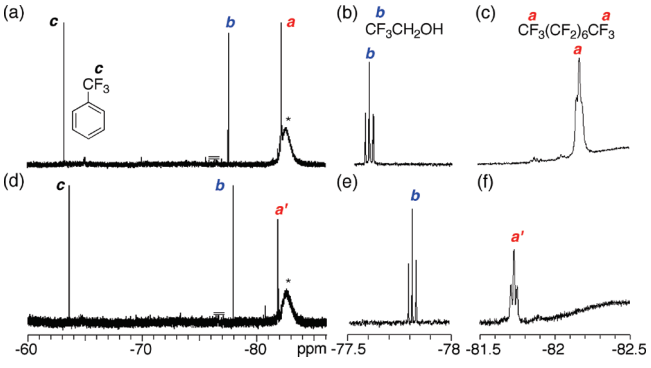

Figure 5. ^{19}F NMR spectra (470 MHz) of PFO, TFMB, and TFE in the presence of **P3** in DMF-d_7 (a−c) and DMF-d_7/$CDCl_3$ (d−f) at 30 °C. (b, c) and (e, f): magnified spectra of (a) and (d), respectively. Asterisk: **P3**-bound fluorine.

interaction, and thereby the more restricted the guest-unit movement. The signal (*a*) was broader with **P4** than with **P1**, indicating the stronger fluorous nature in **P4** than in **P1**, in spite of almost the same fluorine numbers per a single arm: total 120−130 fluorine atoms, either from 13FOMA pendent units in **P4** (n = 10) units or from 12FODMA spacer units in **P1** (l = 6; m = 10); see Scheme 1.

In the presence of the hosts, the CF_3 signal of PFMCH shifted upper field as the core-fluorine (13FOMA) content n increased [(**P1**, **P5**, **P6**) < (**P2**, **P4**) < **P3**], due to the increased electron density within the core. The amounts of entrapped PFMCH in **P2**−**P4** increased with increasing contents of 13FOMA, N_{CF_3} (PFMCH per star: **P2**, 126; **P4**, 236; **P3**, 306: Table S3). Star polymers with the fluorinated linker 12FODMA but without 13FOMA units (**P1**) or with a fluorine free core (**P5**), as well as the linear random polymer (**P6**), were less effective in PFMCH recognition, where the entrapped PFMCH showed sharp multiplets as with free PFMCH in $CDCl_3$ (signal *a* at −70.4 ppm). Thus, the fluorous interaction is highly dependent on the local concentration of the core-bound fluorine pendants in 13FOMA.

P3 could also selectively recognize PFO in the presence of another fluorinated guest (TFMB or TFE); the tip CF_3 signal (*a*) of PFO broadened, while that of TFE remained sharp triplet (*b*) (Figure 5a). Also interesting, the addition of $CDCl_3$ into DMF-d_7 (up to 1/1 v/v) interferes the PFO recognition with **P3** (Figure 5b) and thereby triggers release of once entrapped PFO from the core, as indicated by the reappearance of a sharp triplet of CF_3 (*a*′). This is fully consistent with the rather weak interaction between **P3** and PFO in $CDCl_3$ (Figure S5).

In conclusion, we successfully create fluorous compartments within fluorinated microgel-core star polymers that have directly been synthesized by the ruthenium-catalyzed living radical polymerization. These fluorous-core star polymers efficiently and selectively recognized fluorous compounds even in the presence of hydrophobic and hydrophilic compounds. The unique compartmentalized fluorous environment would contribute to construct new synthetic strategies including stimuli-responsive tandem catalysis and highly selective reactions.

■ ASSOCIATED CONTENT

Supporting Information. Experimental details, characterization, SEC curves, ^{1}H and ^{19}F NMR and ^{19}F DOSY spectra, SEC-MALLS, DLS. This material is available free of charge via the Internet at http://pubs.acs.org.

■ AUTHOR INFORMATION

Corresponding Author

*Tel: +81-75-383-2600. Fax: +81-75-383-2601. E-mail: terashima@living.polym.kyoto-u.ac.jp (T.T.); sawamoto@star.polym.kyoto-u.ac.jp (M.S.).

■ ACKNOWLEDGMENT

This work was partially supported by the Ministry of Education, Science, Sports, and Culture through a Grant-in Aid for Creative Science Research (18GS0209), for which the authors are grateful, and for young scientist (B) (20750091), for which T.T. is grateful.

■ REFERENCES

(1) Bosman, A. W.; Janssen, H. M.; Meijer, E. W. *Chem. Rev.* **1999**, *99*, 1665–1688.
(2) Grayson, S. M.; Fréchet, J. M. J. *Chem. Rev.* **2001**, *101*, 3819–3867.
(3) Van Dongen, S. F. M.; de Hoog, H.-P. M.; Peters, R. J. R. W.; Nallani, M.; Nolte, R. J. M.; van Hest, J. C. M. *Chem. Rev.* **2009**, *109*, 6212–6274.
(4) Gao, H.; Matyjaszewski, K. *Prog. Polym. Sci.* **2009**, *34*, 317–350.
(5) Blencowe, A.; Tan, J. F.; Goh, T. K.; Qiao, G. G. *Polymer* **2009**, *50*, 5–32.
(6) Kanaoka, S.; Sawamoto, M.; Higashimura, T. *Macromolecules* **1992**, *25*, 6414–6418.
(7) Baek, K.-Y.; Kamigaito, M.; Sawamoto, M. *Macromolecules* **2001**, *34*, 215–221.
(8) Baek, K.-Y.; Kamigaito, M.; Sawamoto, M. *Macromolecules* **2002**, *35*, 1493–1498.
(9) Terashima, T.; Kamigaito, M.; Baek, K.-Y.; Ando, T.; Sawamoto, M. *J. Am. Chem. Soc.* **2003**, *125*, 5288–5289.

(10) Terashima, T.; Motokawa, R.; Koizumi, S.; Sawamoto, M.; Kamigaito, M.; Ando, T.; Hashimoto, T. *Macromolecules* **2010**, *43*, 8218–8232.
(11) Bosman, A. W.; Vestberg, R.; Heumann, A.; Fréchet, J. M. J.; Hawker, C. J. *J. Am. Chem. Soc.* **2003**, *125*, 715–728.
(12) Rodionov, V.; Gao, H.; Scroggings, S.; Unruh, D. A.; Avestro, A.-J.; Fréchet, J. M. J. *J. Am. Chem. Soc.* **2010**, *132*, 2570–2572.
(13) Ouchi, M.; Terashima, T.; Sawamoto, M. *Chem. Rev.* **2009**, *109*, 4963–5050.
(14) Matyjaszewski, K.; Tsarevsky, N. V. *Nature Chem.* **2009**, *1*, 276–288.
(15) Rosen, B. M.; Percec, V. *Chem. Rev.* **2009**, *109*, 5069–5119.
(16) Kamigaito, M. *Polym. J.* **2011**, *43*, 105–120.
(17) Bruno, A. *Macromolecules* **2010**, *43*, 10163–10184.
(18) Honda, K.; Morita, M.; Sakata, O.; Sasaki, S.; Takahara, A. *Macromolecules* **2010**, *43*, 454–460.
(19) Horváth, I. T.; Rábai, J. *Science* **1994**, *266*, 72–75.
(20) Curran, D. P. *Angew. Chem., Int. Ed.* **1998**, *37*, 1174–1196.
(21) Yoshida, J.; Itami, K. *Chem. Rev.* **2002**, *102*, 3693–3716.
(22) Sato, S.; Iida, J.; Suzuki, K.; Kawano, M.; Ozeki, T.; Fujita, M. *Science* **2006**, *313*, 1273–1276.
(23) Kraff, M. P. *Adv. Drug Delivery Rev.* **2001**, *47*, 209–228.
(24) Riess, J. G. *Tetrahedron* **2001**, *58*, 4113–4131.
(25) Krafft, M. P.; Riess, J. G. *Chem. Rev.* **2009**, *109*, 1714–1792.
(26) Tsukiji, S.; Miyagawa, M.; Takaoka, Y.; Tamura, T.; Hamachi, I. *Nat. Chem. Biol.* **2009**, *5*, 341–343.
(27) Du, W.; Nystöm, A. M.; Zhang, L.; Powell, K. T.; Li, Y.; Cheng, C.; Wickline, S. A.; Wooley, K. L. *Biomacromolecules* **2008**, *9*, 2826–2833.
(28) Scott, R. L. *J. Am. Chem. Soc.* **1948**, *70*, 4090–4093.
(29) Cohen, Y.; Avram, L.; Frish, L. *Angew. Chem., Int. Ed.* **2005**, *44*, 520–554.